Journal of Plant Research (2021) 134:765–778
https://doi.org/10.1007/s10265-021-01292-6

REGULAR PAPER – TAXONOMY/PHYLOGENETICS/EVOLUTIONARY BIOLOGY

# Acropetally developing vascular bundles coexisting with basipetally developing and basally blindly ended vascular bundles in scapes of *Eriocaulon taquetii* (Eriocaulaceae, monocotyledons)

**Yasuhiko Endo**[1] · **Fumiya Sugawara**[1] · **Katsuhiro Yashiro**[2]

Received: 27 November 2020 / Accepted: 27 March 2021 / Published online: 9 April 2021


**Abstract**
In various monocotyledons, there are basally blindly ended stem vascular bundles, which never connect to the vascular bundles of roots. These blindly ended vascular bundles seem to be unsuitable for transferring water in terrestrial plants. In the present study, we aim to clarify the trace of the blindly ended stem vascular bundles in whole plants, and consider the evolutional process for holding such vascular bundles in the stem. We examined a whole stem vasculature of *Eriocaulon taquetii* (Eriocaulaceae, monocotyledons) by observation of serial transverse sections, cut by a manual rotary microtome, and viewed under an epifluorescence microscope. Our investigation revealed a threedimensional reconfiguration of the scape vasculature and detected basipetally developing and basally blindly ended vascular bundles, originated from involucral bracts and arranged with acropetally developing vascular bundles alternately in the scape internode. The basipetally developing and basally blindly ended vascular bundles, which originate from the primodia of foliar organs, have been reported in various commelinids. The characteristic vascular bundles would be homologous and presumed to be a synapomorphy of commelinids. These vascular bundles are considered to be a relic characteristic from ancestral semiaquatic plants of monocotyledons.

**Keywords** Acropetally developing · Basipetally developing · Blindly ended vascular bundle · *Eriocaulon taquetii* · Monocotyledon · Synapomorphy

## Introduction

Monocotyledons have been presumed to be monophyletic and nested in dicotyledons on the molecular phylogenetic tree of angiosperms (APG IV 2016). This fact may mean that the characteristics, shared by various monocotyledons and different from those of dicotyledons, are synapomorphies of monocotyledons.

One such characteristic is related to the stem vascular systems, i.e., monocotyledonous stems have many scattered primary 'vascular bundles' (abbreviated as VBs) in the transverse sections, but dicotyledonous stems have primary VBs arranged in a single ring (Gifford and Foster 1989; Heywood 1978). However, there are some exceptions in monocotyledons, e.g., small monocotyledons, such as plants of the Mayacaceae (Poales), Petrosaviaceae (Petrosaviales), and Eriocaulaceae (Poales), have VBs arranged in a ring in transverse stem sections (Zimmermann and Tomlinson 1972). This arrangement of stem VBs was considered to be the result of a reduction leading to a simplified stem vascular system (Zimmermann and Tomlinson 1972).

On the other hand, in monocotyledonous species, characteristic VBs, different to those of dicotyledons, have been reported as follows: (1) Commelinaceae species (Commelinales) have VBs, which were considered to be differentiated from intercalary meristems, and end in a "blind spot" (Vita et al. 2019); (2) *Alpinia speciosa* L. (Zingiberaceae, Zingiberales) has an inner and outer system of leaf traces at the apex of the aerial vegetative axis, and the inner system is more developed than the outer one (differentiating both basipetally and basifugally) (Bell 1980); (3) *Zea mays* L. (Gramineae, Poales) has smaller basipetally developing VBs starting at the bases of leaves (Bosabalidis et al. 1994; Sharman 1942); (4) *Eleocharis acuta* R. Br. (Cyperaceae, Poales) has smaller VBs in haulms, and the tissues of the smaller VBs are undifferentiated at the

✉ Yasuhiko Endo
yasuhiko.endo.sci@vc.ibaraki.ac.jp

[1] Graduate School of Science and Engineering, Ibaraki University, Bunkyo 2-1-1, Mito 310-8512, Japan

[2] Karabe 4-26-38, Narita 286-0036, Japan

base of the haulms (Evans 1965); (5) *Prionium serratum* (L. f.) Drège (Juncaceae, Poales) also has similar blindly ended stem cortical VBs (Zimmermann and Tomlinson 1968); (6) *Cyperus alternifolius* L. (Cyperaceae, Poales) has smaller bundles in the culms, and the smaller bundles are discontinuous with rhizome bundles and end blindly at the base of the internode (Fischer 1970); (7) *Oriza sativa* L. (Gramineae, Poales) has small VBs that end blindly at the base of leaf blade (Chonan et al. 1974); (8) *Calamus longipinna* K. Schum. & Lauterb. (Arecaceae, Arecales) has basipetal and blindly ended axial VBs (Tomlinson and Spangler 2002; Tomlinson et al. 2001); (9) *Rhapis excelsa* (Thunb.) A. Henry (Arecaceae, Arecales) has minor leaf traces, which become smaller and end blindly further up the stem (Zimmerman and Tomlinson 1965). These characteristic VBs of monocotyledons seem to be similar to each other because almost all of these VBs are basipetally developing and basally blindly ended.

In eudicotyledons also, there are basipetally developing primary VBs originated from the base of the primordia of foliar organs (Claßen-Bockhoff et al. 2020). However, the primary VBs of eudicotyledons immediately connected to the neighbouring VBs (Claßen-Bockhoff et al. 2020). This means that these eudicotyledonous stem VBs would not end blindly at the basal end. Therefore, the basally ending of the primary VBs might be a synapomorphy of monocotyledons.

In the present study, we aim to clarify the route and the relationships with other VBs of basally blindly ended VBs in monocotyledons by tracing the vasculatures. However, the tracing has been considered to be challenging because of many scattered stem VBs in most monocotyledons (Tomlinson 1995; Zimmerman and Tomlinson 1972). So, we analyzed the vasculature of whole stems and leaves of a monocotyledonous species, *Eriocaulon taquetii* L. (Eriocaulaceae, Poales), because *Eriocaulon taquetii* was observed to have only six (or eight) scape VBs arranged in a ring in our preliminary study, and was considered to have simplified vascular systems. The monocotyledonous family Eriocaulaceae has stems, composed of scapes and rhizomes, and foliar organs, i.e., involucral bracts, spathes (leaf-sheaths), and foliage leaves attached to rhizomes (Stützel 1998; Tomlinson 1969). It has been clarified that the VBs of scapes are usually arranged in double rings, and those of rhizomes are discrete and diffusely distributed (Scatena and Giulietti 1996; Scatena and Rosa 2001; Scatena et al. 1999, 2004, 2005; Stützel 1998; Tomlinson 1969). However, it has not been clarified which VBs are basipetally developing and blindly ended.

## Materials and methods

### Plant materials

The materials (*Eriocaulon taquetii* Lecomte) were collected in a marsh (at Higashinaruse-mura, Ogachi-gun, Akita Prefecture, Japan) and the voucher specimen, 'Endo & Takada 3925', was deposited in the herbarium of Ibaraki Nature Museum (INM). The samples were fixed in FAA (formaldehyde: acetic acid: 50% aqueous ethanol = 0.5: 0.5: 9.0) in the fields. The identification of these materials referred to Takada (2017).

### Histological study

The thin serial transverse sections (approximately 4–7 µm thick) of the stems (including scapes and rhizomes) were made using a standard paraffin sectioning method with an RX-860 microtome (Yamato Kohki Industrial Co. Ltd., Saitama, Japan). The sections were stained with safranin, fastgreen FCF, and Heidenhein's hematoxylin and then observed under a Nikon Eclipse Ni-U epifluorescence microscope with a fluorescence filter cube G-2A C-FL (Nikon Co. Ltd., Tokyo, Japan). This filter cube employs an excitation passband from 510 to 560 nm (green excitation) and was combined with a 590 nm cut-on wavelength (longer wavelengths than those in the yellow region; i.e., ≥ 590 nm) emission filter. Under the green excitation, the parts stained with safranin would fluoresce (Bond et al. 2008), and these are the lignified regions (Bond et al. 2008). The chloroplasts also fluoresce under the excitation (Nikon Instruments Inc. 2020).

The names of the organs and tissues, used in the description of the present study, are according to Hare (1945) and Stützel (1998).

## Results

### Outer morphology (Fig. 1)

The most apical part of the mature plant of *Eriocaulon taquetii* is the head, i.e., a capitulum. The head has approximately six flowers (three female flowers and three more apically arranged male flowers) and is supported by a three- or four-angled scape (less than 11 cm long). The basal part of the scape connects to a rhizome (about 5 mm long). The basal part of the head is subtended by involucral bracts (about 4–5 mm long), and the basal part of the scape is subtended by a spathe (a leaf-sheath, about

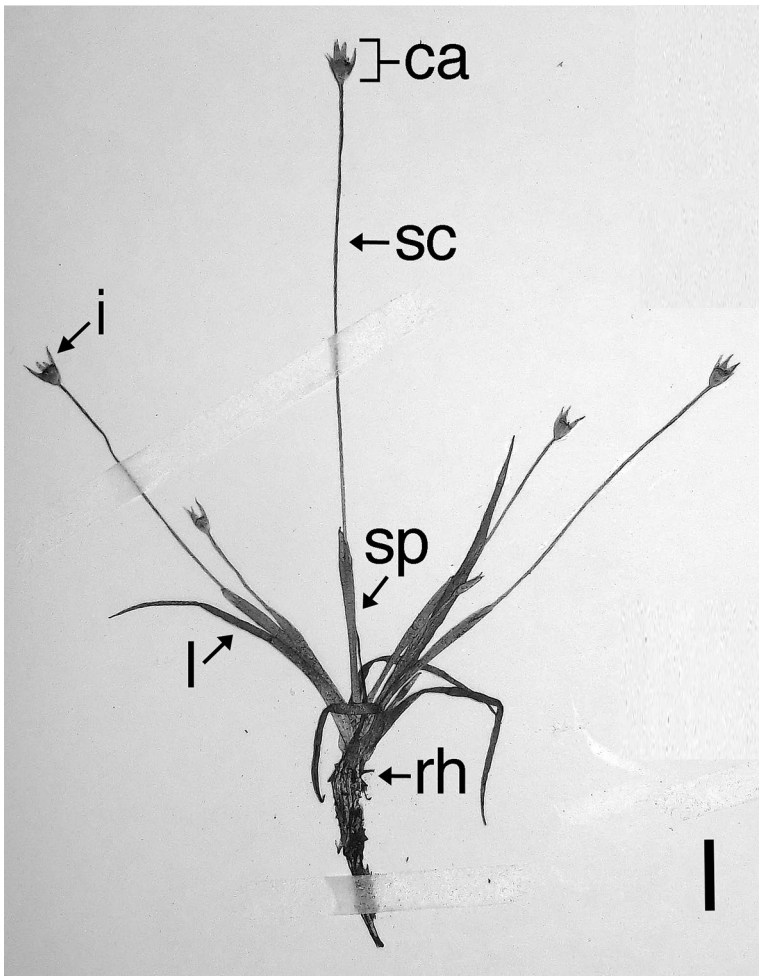


**Fig. 1** Photograph of a herbarium specimens of *Eriocaulon taquetii* with five scapes. *ca* capitula, *i* involucral bract, *l* leaf, *rh* rhizome, *sc* scape, *sp* spathe. *Scale bar* 1 cm

20–25 mm long). The rhizome has lanceolate leaves (less than 50 mm long) and adventitious roots.

## Histological features in transverse sections

The differences in the arrangements, sizes, and shapes of the stem VBs between the different portions of the stems (from the scape to the rhizome) of *Eriocaulon taquetii* are described as follows, based on the transverse serial sections of the scape and rhizome (Figs. 2,3,4,5). Schematic diagrams of the sections of the scape are shown in Fig. 6, and a diagram of the vasculature is shown in Fig. 7.

In the individuals examined, there were two types of scapes, three-angled scapes and four-angled ones. In the following description, we refer to the three-angled scapes for convenience because they had fewer VBs than the four-angled ones. However, we could not find any difference between the two types of scapes in the arrangement of VBs (apart from the differences in the numbers of VBs).

In the following description, the transverse section is described from the apical part to the basal part of the plant.

(1) At the basal portion of the head, subtended by three involucral bracts (Figs. 2a–c, 6a).

In the transverse section, there are three involucral bracts at the peripheral part and six sets of tissues composed of smaller cells at the center (Fig. 2a). The outer ring is composed of three band-shaped tissues and the inner ring of three disk-shaped tissues (Fig. 2b). These tissues were considered to be VBs because of the connection to the more basal VBs (Fig. 2e, f). These bundles include the separately arranged cells, with cell walls that fluoresce under an epifluorescence microscope (Fig. 2c). These cells may be more lignified than the other surrounding smaller cells because of the property of fluorescing of such lignified portions (Bond et al. 2008) and were considered to be the walls of the vessels. In the disk-shaped inner VBs, the vessels are situated radially inside the disk (Fig. 2c), and the bundles would, therefore, be collateral VBs. On the other hand, in the band-shaped outer VBs, the vessels are situated radially inside and outside (Fig. 2c). Therefore, the bundles would be amphivasal VBs.

We observed that the disk-shaped inner three VBs lead up to the peduncle of the head (Fig. 7p1–p3), and

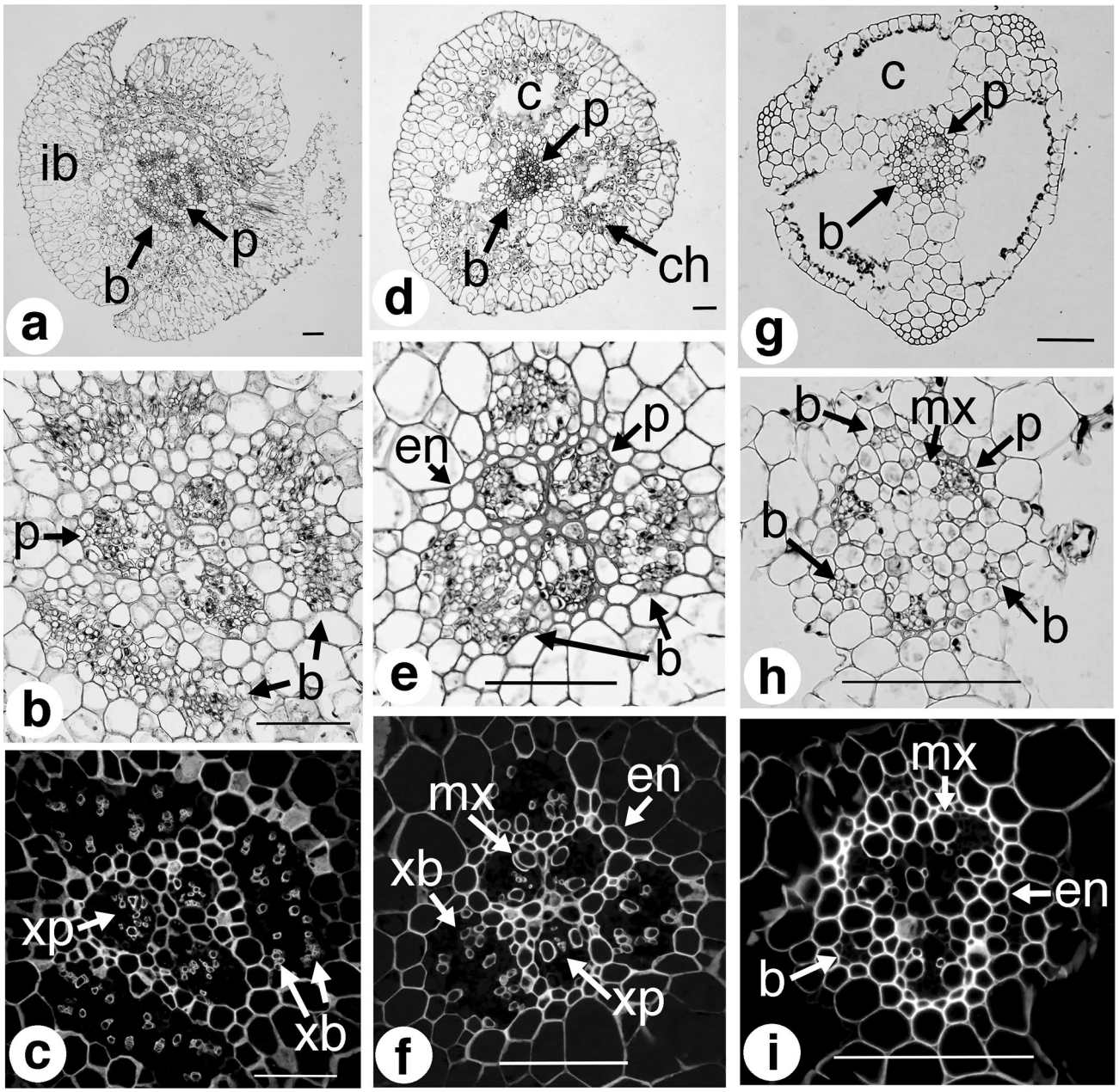


**Fig. 2** Transverse sections of scapes of *Eriocaulon taquetii*. **a** At the basal portion of the capitula, attaching three involucral bracts. **b**, **c** Enlargement of the central part of the section '**a**', showing central cylinder, composed of three primary collateral VBs, and surrounding three band-shaped amphivasal VBs. **d** Just under the capitula. **e**, **f** Enlargement of the central part of the section '**d**', showing central cylinder, composed of three primary collateral VBs, and surrounding three collateral VBs. **g** At the middle part of the scape. **h**, **i** Enlargement of the central part of the section '**g**', showing central cylinder composed of three primary collateral VBs, and surrounding three slender immature VBs. **a**, **b**, **d**, **e**, **g**, **h** Photographs taken under a light microscope. **c**, **f**, **i** Photographs taken under an epifluorescence microscope. *b* VB surrounding central cylinder, *c* air canal, *ch* chlorenchyma, *en* endodermis, *ib* involucral bract, *mx* metaxylem, *p* VB of central cylinder, *xb* xylem of amphivasal VB, *xp* xylem of collateral VB. *Scale bars* 0.1 mm

the band-shaped outer three bundles lead to the involucral bracts at the more apical part (Fig. 7b1–b3).

The disk-shaped inner three VBs are surrounded by parenchyma cells, with cell walls fluorescing significantly (Fig. 2c). These parenchyma cells would have more lignified cell walls, surround the central VBs in the peduncle, and form an endodermis.

(2) Just under the involucral bracts (Figs. 2d–f, 6b).

In the transverse section, there are three spaces, i.e., air canals (air-lacunae), at the cortex (Fig. 2d). The air

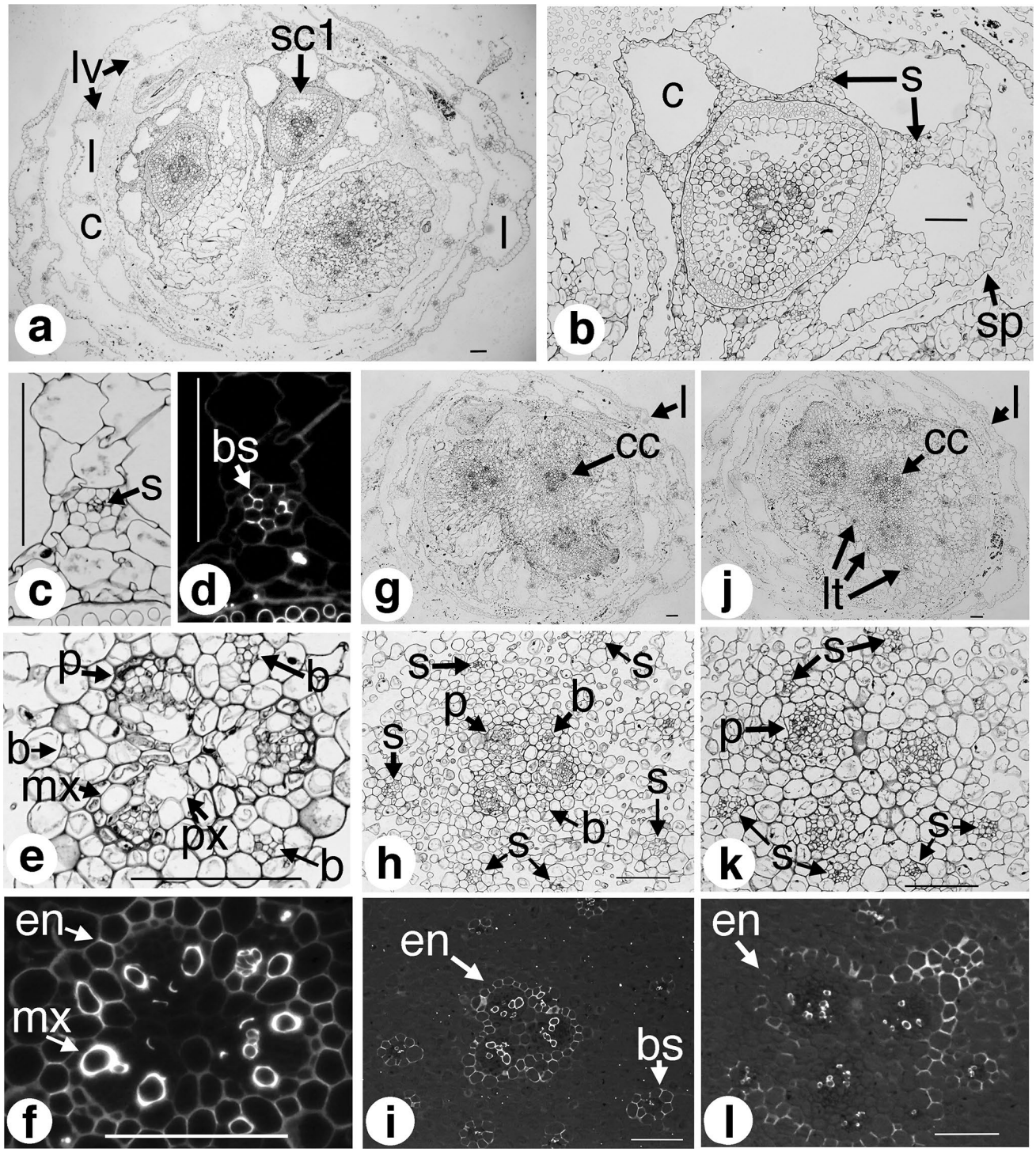


**Fig. 3** Transverse sections of basal parts of scapes (an apical part of a rhizome) of *Eriocaulon taquetii*. **a** Basal part of three scapes, growing from one rhizome, each surrounded by a spathe and wholly surrounded by four rhizomal leaves. **b** Enlargement of the 'sc1′ of '**a**', surrounded by a spathe. **c, d** One of the boundaries between air canals of spathe in '**b**'. **e**, **f** Central cylinder of the 'sc1′ in '**a**', composed of three collateral primary VBs, and closely surrounding three immature VBs. **g** more basal part than '**a**', without air canal of spathes. **h, i** Enlargement of the central cylinder of '**g**' leading to 'sc1′ of '**a**', showing three collateral primary VBs of the 'cc', closely surrounding two immature VBs, and six spathe VBs at outer side. **j** More basal part of the three scapes than '**g**', showing leaf traces in rhizome. **k, l** Enlargement of 'cc' of '**j**', showing three larger VBs of central cylinder, surrounding six smaller spathe VBs, of which one located inside of the endodermis. **a**–**c**, **e**, **g**, **h**, **j**, **k** Photographs taken under a light microscope. **d**, **f**, **i**, **l** Photographs taken under an epifluorescence microscope. *b* immature VB surrounding central cylinder. *bs* bundle sheath, *c* air canal, *cc* central cylinder, *en* endodermis, *l* leaf, *lt* leaf trace, *lv* VB of leaf, *mx* metaxylem, *p* VB of central cylinder, *px* protoxylem, *s* VB of spathe, *sc1* first scape, *sp* spathe. *Scale bars* 0.1 mm

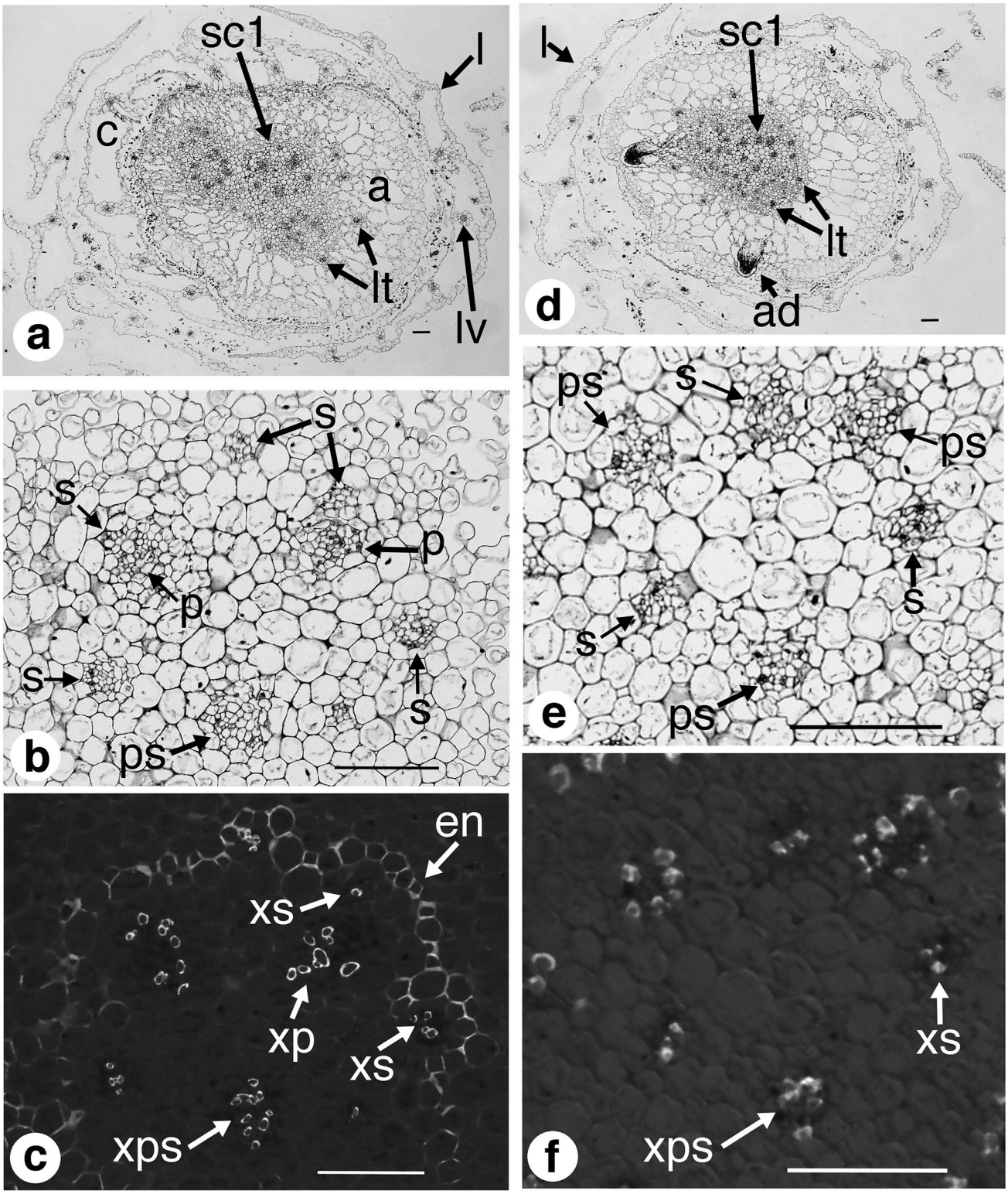


canals are irregularly embedded by chlorenchyma at the peripheral region (Fig. 2d). The air canal is facing the disc-shaped amphivasal VBs, which lead to the involucral bracts (Fig. 2d–f). The three innermost VBs are collateral VBs (Fig. 2e) and lead to the peduncle of the head (Fig. 7p1–p3). These three VBs are surrounded by an endodermis (Fig. 2e, f).

(3) At the middle part of the scape (Figs. 2g–i, 6c).

In the transverse section, there are three corners with sclerenchyma (Fig. 2g). In the cortex, there are wider air canals

◂**Fig. 4** Transverse sections of a rhizome of *Eriocaulon taquetii*. **a** More basal part than **Fig. 3j**, showing three scapes wholly surrounded by aerenchymae. **b, c** Enlargement of the central cylinder of 'sc1′, showing three larger primary VBs, of which one closely approaches to spathe VB, and another adnates to another spathe VB. **d** More basal part than **a**, showing adventitious roots, scape VBs and leaf traces, gathering into the center. **e**, **f** Enlargement of 'sc1′ in **d**, showing three larger scape VBs and three slender spathe VBs. **a**, **b**, **d**, **e** Photographs taken under a light microscope. **c**, **f** Photographs taken under an epifluorescence microscope. *a* aerenchyma, *ad* adventitious root, *c* air canal, *en* endodermis, *l* leaf, *lt* leaf trace, *lv* VB of leaf, *p* VB of scape central cylinder, *ps* VB leading to a peduncle and a spathe, *s* VB of a spathe, *sc1* first scape, *xs* xylem of the VB of spathe, *xp* xylem of the vascular bundle leading to peduncle, *xps* xylem of the VB leading to a peduncle and a spathe. *Scale bars* 0.1 mm

than those at the more apical part (Fig. 2g). In the center, there are three collateral VBs, surrounded by an endodermis, which lead to the peduncle of the head (Fig. 2h, i). Just outside the central cylinder (sensu Oliveira et al. 2015), there are three smaller cell groups (Fig. 2h-b). These cell-groups lead to the VBs of the involucral bracts (Fig. 7b1–b3) and would be the undifferentiated tissues of the VBs. These VBs would be larger and more differentiated at the more apical part of the scape.

(4) At the upper part of the scape basal node (Figs. 3a–f, 6d).

In the transverse section of the basal part of the scape, there are sections of foliage leaves (attached to the rhizome), spathes, and scapes (Fig. 3a). The foliage leaves and spathes have air canals and VBs (Fig. 3a). The VBs are located at each boundary between the air canals (Fig. 3a, b, c). These VBs have a bundle-sheath (Fig. 3c, d).

At the center of the scape, there are three collateral VBs, surrounded by an endodermis, which lead to the peduncle (Fig. 7p1–p3) and form a central cylinder (Fig. 3e, f). Near the central cylinder, there are three cell groups comprising smaller cells (Fig. 3e). These cell groups would lead to the involucral bract VBs (Fig. 7b1–b3).

(5) At the scape basal node (Figs. 3g–i, 6e).

In the transverse section of the rhizome (Fig. 3g), the scapes join, and the central cylinder, enclosed by an endodermis, is surrounded by spathe traces (Fig. 3h-s) (each surrounded by a bundle sheath, Fig. 3i-bs). Near the central cylinder, there are two traces of VBs (enclosed by a bundle sheath) (Fig. 3h-b), which lead to the involucral bracts (Fig. 7b).

Between the central cylinders of the scapes, there are net-like tissues (aerenchyma), which have many spaces between the cell rows (Fig. 3g).

(6) Just under the basal node of the scape (Fig. 3j–l).

Here, around three scape central cylinders become closer to each other (Fig. 3j) but are individually enclosed by an endodermis (Fig. 3l-en). Between the scape central cylinders, there is almost no net-like aerenchyma (Fig. 3j). On the other hand, the group of the scape central cylinders is wholly surrounded by aerenchyma (Fig. 3j).

One of the central cylinders is surrounded by spathe traces (Fig. 3k-s), and the central cylinder and several spathe traces are enclosed by an endodermis (Fig. 3k, l-en). The rest of the spathe traces are individually enclosed by a bundle-sheath (Fig. 3k, l). Notably, the involucral bract traces (Fig. 7b1–b3), which should be present at the upper part of the scape (Fig. 3b–h) and near the VBs leading to the peduncle of the head, could not be observed (Fig. 3k, l).

There are leaf traces at the cortex, including aerenchyma (Fig. 3j-lt).

(7) At the rhizome where spathe traces branch from the central cylinder VBs (Figs. 4a–c, 6f, 7).

The central cylinders of the scapes (Fig. 4a-sc1), each enclosed by an endodermis (Fig. 4c-en), are composed of VBs that lead to the peduncle of the head and the spathe traces (Figs. 4b, c; 6f; 7p, s). Several spathe traces branch from the VBs, leading to the peduncle of the head (Figs. 4b, c; 6-sb1, -sb2, -sb3; 7-sb1, -sb2, -sb3).

In the rhizome cortex, the leaf traces are nearer to the central cylinder (Fig. 4d-lt) than those at the more apical part (Fig. 4a-lt).

(8) At the rhizome more basal than (7) (Figs. 4d–f, 6g, 7).

All central cylinders of the three scapes are adjacent to each other and enclosed by an endodermis (Fig. 4d). The most developed central cylinder of the three is observed to be composed of six VBs (Fig. 4e, f). Three lead to the peduncle of the head (larger xylems 'xps' in Fig. 4f) (Figs. 6g-p1(sb1), -p2(sb2), -p3(sb3); 7-p1(sb1), -p2(sb2), -p3(sb3)), and the other three are spathe traces (smaller xylems 'xs' in Fig. 4f) (Figs. 6-s1, -s2, -s3; 7-s1, -s2, -s3).

Several leaf traces are located in the central cylinders, enclosed by an endodermis, and are outside the traces of the peduncle of the head and spathe (Fig. 4d).

The tissues of the adventitious roots are adjacent to the central cylinder (Fig. 4d).

(9) At the rhizome more basal than (8) (Fig. 5a–f).

The VBs are scattered in the disk-shaped central cylinder. Several leaf traces, with a bundle sheath, are located at the boundary between the cortex and the central cylinder, i.e., at the endodermis (Fig. 5b-lt, c-bs). At the more basal part, these leaf traces are located inside the endodermis (Fig. 5e-lt, f-bs).

(10) At the rhizome more basal than (9) (Fig. 5g–i).

The VBs just inside the endodermis are arranged in a ring. These VBs would be collateral VBs with the phloem inside and the xylem outside (Fig. 5g–i). Inside the ring of these VBs, there is another ring with fewer VBs surrounding parenchyma. Therefore, the central cylinder appears to consist of double rings of VBs.

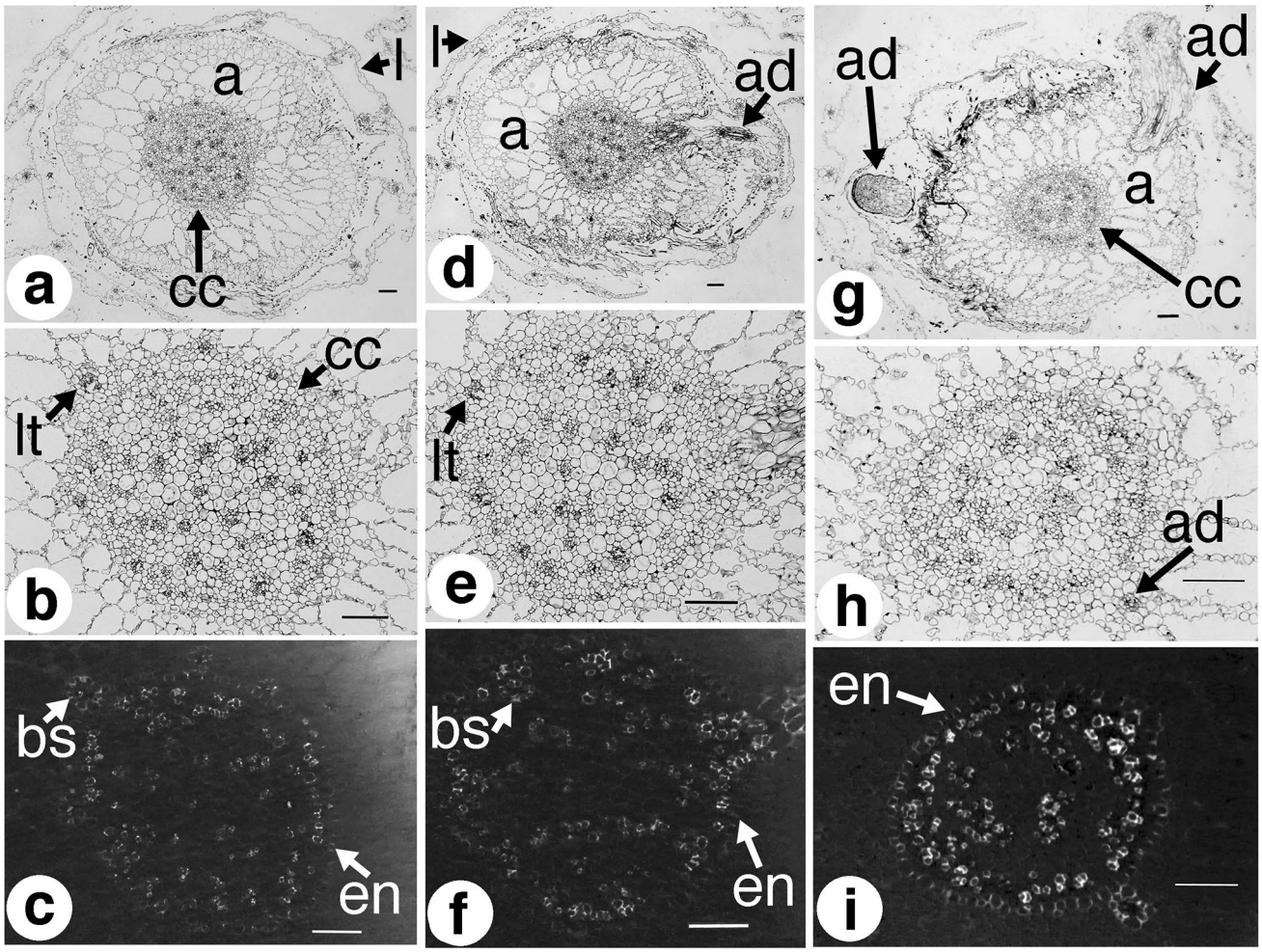


**Fig. 5** Transverse sections of a basal part of rhizome of *Eriocaulon taquetii*. **a** More basal part than **Fig. 4d**, showing scape VBs gathering and forming larger central cylinder, surrounded by aerenchyma. **b**, **c** Enlargement of central cylinder (atactostele) in '**a**', with leaf traces situated at the boundary between cortex (aerenchyma) and a central cylinder. **d** More basal part than '**a**' with adventitious root originated from central cylinder. **e**, **f** Enlargement of central cylinder (atactostele) in '**d**', with leaf traces situated inside of the endodermis. **g** More basal part than '**d**'. **h**, **i** Enlargement of central cylinder of '**g**', with collateral VBs wholly surrounding the central cylinder, composed of a ring of VBs. **a**, **b**, **d**, **e**, **g**, **h** Photographs taken under a light microscope. **c**, **f**, **i** Photographs taken under an epifluorescence microscope. *a* aerenchyma, *ad* adventitious root, *bs* bundle sheath, *cc* central cylinder, *en* endodermis, *l* leaf, *lt* leaf trace. *Scale bars* 0.1 mm

Courses of VBs connected to heads, involucral bracts, spathes, and foliage leaves of *Eriocaulon taquetii.*

Just under the basal node of the scape, there are six VBs arranged in a ring (Figs. 6g, 7). In these six bundles, three bundles branch into two each, i.e., an inner one and an outer one, at the basal node of the scape (Figs. 6f-p1(sb1), -p2(sb2), -p3(sb3); 7-p1(sb1), -p2(sb2), -p3(sb3)). The outer three bundles enter into a spathe (Figs. 6e-sb1, -sb2, -sb3; 7-sb1, -sb2, -sb3), and the inner three lead to the peduncle of the head through the scape (Figs. 6e-p1, -p2, -p3; 7-p1, -p2, -p3). The other three of the six enter into a spathe (a leaf-sheath) (Figs. 6e-s1, -s2, -s3; 7-s1, -s2, -s3). Inside these three spathe VBs, the other three bundles appear suddenly just over the scape's basal node. These bundles connected to the involucral bracts at the apical node of the scape (Figs. 6d-b1, -b2, -b3; 7-b1, -b2, -b3).

Several leaf traces, arranged in an arc, suddenly appear at the peripheral region of the central cylinders, i.e., inside the endodermis but outside the VBs, leading to the peduncles of the heads and spathes, in the rhizome (Fig. 4d). Then, the leaf traces run into the cortex over the endodermis and are surrounded by a bundle sheath at the more apical part of the rhizome (Fig. 4a). These traces enter into a foliage leaf attached to the rhizome (Fig. 3a).

## Discussion

Basally blindly ended and basipetally developing VBs originated from the base of primordia of involucral bracts in *Eriocaulon taquetii.*

The scape internodal VBs, leading to the involucral bract, basally ended blindly just over the scape's basal node (Fig. 7). The basally terminal tissues are composed of smaller undifferentiated cells (Fig. 3h, i). On the other hand, the VB becomes thicker and more differentiated towards the apical part. Therefore, this is a basipetally developing and basally blindly ended VB, characteristic of monocotyledons. This appearance of the involucral bract VBs is similar to the small bundles appearing at the basal parts of the internodes of the scapose aerial shoot (haulm) of *Eleocharis acuta* (Cyperaceae), reported by Evans (1965). These bundles are considered to originate from the internodal intercalary meristems (sensu Fischer and French 1976; Pereira and Rodrigues 2012), because the most basal end of the VB tissue is undifferentiated (Evans 1965). However, in eudicotyledons (one of the sister groups of monocotyledons), basipetally developing VBs are originated from the basal parts of primordia of foliar organs (Claßen-Bockhoff et al. 2020). Therefore, we consider that the basally blindly ended basipetal developing VBs are originated from the bases of primordia of involucral bracts in *Eriocaulon taquetii*. On the other hand, there are VBs, leading to the peduncle of the head, which pass through the apical and basal nodes of the scapes and enter into the rhizome (Figs. 6-p1, -p2, -p3; 7-p1, -p2, -p3). These peduncular VBs seem to elongate to the stem apical meristem, which generate procambium (Esau 1953; Maze 1977; Scarpella and Meijer 2004), and are acropetally developing VBs (sensu Aloni 2010). Consequently, there are two types of VBs, i.e., acropetally developing or basipetally developing VBs, in the scape of *E. taquetii*. The acropetally developing VBs were thicker than the basipetally developing ones at the basal half of the scape but similar at the apical part. The acropetally developing VBs and basipetally developing ones were arranged alternately. The acropetally developing VBs each branched into a scape VB and a spathe VB. Such branching has not been reported in previous histological studies on *Eriocaulon* species, e.g., by Hare (1945), Holm (1901), Scatena et al. (1999, 2005), Stüzel (1998), and Tomlinson (1969).

The basipetally developing and blindly ended VBs are positioned around the acropetally developing VBs in stems, and usually, the former VBs are slenderer than the latter VBs. The former VBs are considered to have developed later than the latter (Bell 1980; Vita et al. 2019). The former VBs have been observed at least in commelinids, i.e. including Zingiberales, Commelinales, Poales and Arecales (APG IV 2016; Stevens 2001). Therefore, the presence of the former VBs could support a presumption that this characteristic VB is a synapomorphy of commelinids.

The characteristic VBs appear separately just over the nodes, and may contribute to an increase in the numbers of stem VBs. Therefore, they also contribute to the characteristic stem vascular system, i.e. an atactostele, of commelinids.

Other organs having basally blindly ended VBs in *Eriocaulon taquetii.*

We detected several leaf traces arranged in an arc between the central cylinder and endodermis in the transverse section of rhizomes. These leaf traces appeared suddenly and seemed to be basally blindly ended. However, it is not clear whether these traces are basipetally developing or not.

In the six spathe (leaf-sheath) traces, two types of VBs, located alternately, were observed, i.e., branching type (Fig. 7-sb1, -sb2, -sb3) and non-branching type (Fig. 7-s1, -s2, -s3). The xylems of non-branching type VBs were smaller than those of the branching type (Fig. 4f). When two types of VBs, i.e., smaller VBs and larger ones, run through organs side by side, generally smaller ones are basipetally developing VBs in some monocotyledons, e.g., maize (Bosabalidis et al. 1994) and rice (Chonan et al. 1974). Therefore, the smaller and non-branching type spathe VBs are considered to be basipetally developing ones. However, we could not find tissues composed of undifferentiated smaller cells at the basal terminals of the smaller three spathe VBs.

At the most basal part of rhizomes of *Eriocaulon taquetii*, we found a ring of collateral VBs. This ring would be generated from the primary thickening meristem (reviewed by Rudall 1991). Such meristems were reported in Xyridaceae by Sajo (1999) and in Cyperaceae by Rodrigues and Estelita (2009).

We consider that almost half of the VBs of *Eriocaulon taquetii* are basipetally developing, blindly ended, and originated from the primordia of foliar organs.

Basally blindly ended VBs in angiosperms.

Basally blindly ended primary VBs in stems of dicotyledonous plants may never have been reported. The reasons may be that such VBs originated from the bases of foliar organs adnate to the neighboring VBs (Bayer et al. 2009; Claßen-Bockhoff et al. 2020) and formation of secondary VBs through the vascular cambium (Povilus et al. 2020). The secondary VBs may mask the trace of the primary VBs. On the other hand, the vascular cambium is absent in monocotyledons (Povilus et al. 2020). Therefore, the traces of primary VBs are able to be recognized.

Basally blindly ended VBs seem to be unsuitable for transferring of water absorbed by subterranean roots in terrestrial monocotyledonous plants. However, the blindly ended VBs originated from the primordia of foliar organs would be useful for transport of photosynthetic products

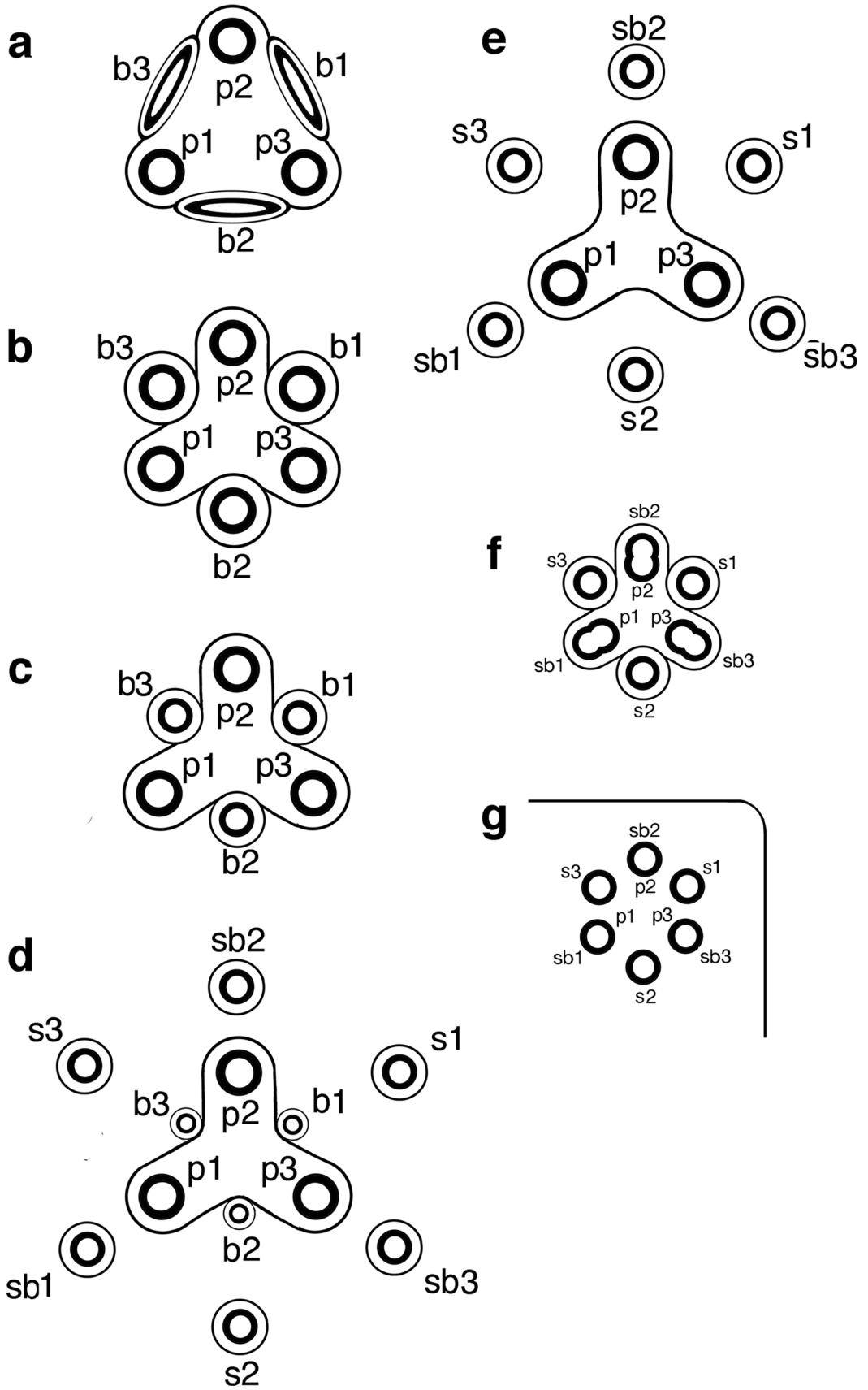
a
b3
b1
p2
p1
p3
b2
b
b3
b1
p2
p1
p3
b2
c
b3
b1
p2
p1
p3
b2
d
sb2
s3
s1
b3
p2
b1
p1
p3
b2
sb1
sb3
s2
e
sb2
s3
s1
p2
p1
p3
sb1
sb3
s2
f
sb2
s3
s1
p2
p1
p3
sb1
sb3
s2
g
sb2
s3
s1
p2
p1
p3
sb1
sb3
s2

◂**Fig. 6** Schematic diagrams of scape transverse sections of *Eriocaulon taquetii*, indicating the numbers, positions, and shapes of VBs and the presence or absence of an endodermis and a bundle-sheath. **a** At the basal portion of the capitula, drawn based on Fig. 2b, c of the present study. **b** Just under the capitula, drawn based on Fig. 2e, f. **c** At the middle of the scape, drawn based on Fig. 2h, i. **d** At the basal part of the scape surrounded by involucral bract VBs and spathe VBs, drawn based on Fig. 3h, i. **e** At the apical part of the rhizome, drawn based on Fig. 3k, l. **f** At the apical part of the rhizome but more towards the base than the position of '**e**', drawn based on Fig. 4b, c. **g** At the portion of the rhizome in which VBs of all scapes are surrounded by one endodermal layer, drawn based on Fig. 4e, f. The portions enclosed by thicker lines indicate positions of VBs. The thinner lines indicate an endodermal layer or VB sheaths. *b1–b3* VB connected to involucral bract, *p1–p3* VB connected to peduncle, *s1–s3* VB connected to spathe, *sb1–sb3* VB branched from *p1–p3* and connected to spathe. The same abbreviations and numbers indicate connections between the VBs of different transverse sections

from the foliar organs to the stems, at least. In addition, the monocotyledons are presumed to have a common semiaquatic ancestor (Givnish et al. 2018; Povilus et al. 2020). Therefore, such basally blindly ending VBs, useful for transferring photosynthetic products but unsuitable for transferring of water, might persist as a characteristic acquired during the semiaquatic life of a monocotyledonous ancestor.

Monocotyledons have been presumed to be monophyletic and to consist of 11 monophyletic orders based on molecular phylogenetic studies (APG IV 2016). The monocotyledonous characteristic VBs have been detected in plants of four orders of commelinids (a part of monocotyledons) as mentioned above. However, they may not have been detected in other monocotyledonous plants (the remaining seven orders, i.e., Acorales, Alismatales, Petrosaviales, Dioscoreales, Pandanales, Asparagales, and Liliales). In these seven orders, inner large VBs and outer small ones (which may be developing basipetally and blindly ended) could be observed in rhizomes of Acorales species, i.e., *Acorus caramus* L. and *A. gramineus* Sol. ex Aiton observed by Saikawa (2016); Alismatales spp., i.e. leaf petioles of Alismataceae spp. observed by Stant (1964), peduncles of *Sagittaria guayanensis* H. B. K. ssp. *lappula* (D. Don) Bogin observed by Govindarajalu (1967), and leaf petioles of *Sagittaria sagittifolia* L. observed by Bercu (2005); Dioscoreales spp., i.e., stems of Dioscoreales spp. reported by Ayensu (1972), stems of *Dioscorea* spp. observed by Sheikh and Kumar (2017), stems of *D. sansibarensis* Pax observed by Tan and Rao (1974), and stems of *D. tokoro* Makino observed by Saikawa (2016); and Asparagales spp., i.e., leaves of Agavaceae spp. observed by Bluden and Jewers (1973), leaves of *Yucca glauca* Nutt. observed by Blunden and Binns (1970), and stems of *Asparagus officinalis* L. observed by Harb et al. (2016). To know the distribution of the characteristic VBs in monocotyledons precisely, we need further investigations about the presence or absence of the VBs especially in the monocotyledonous plants of the remaining seven orders.

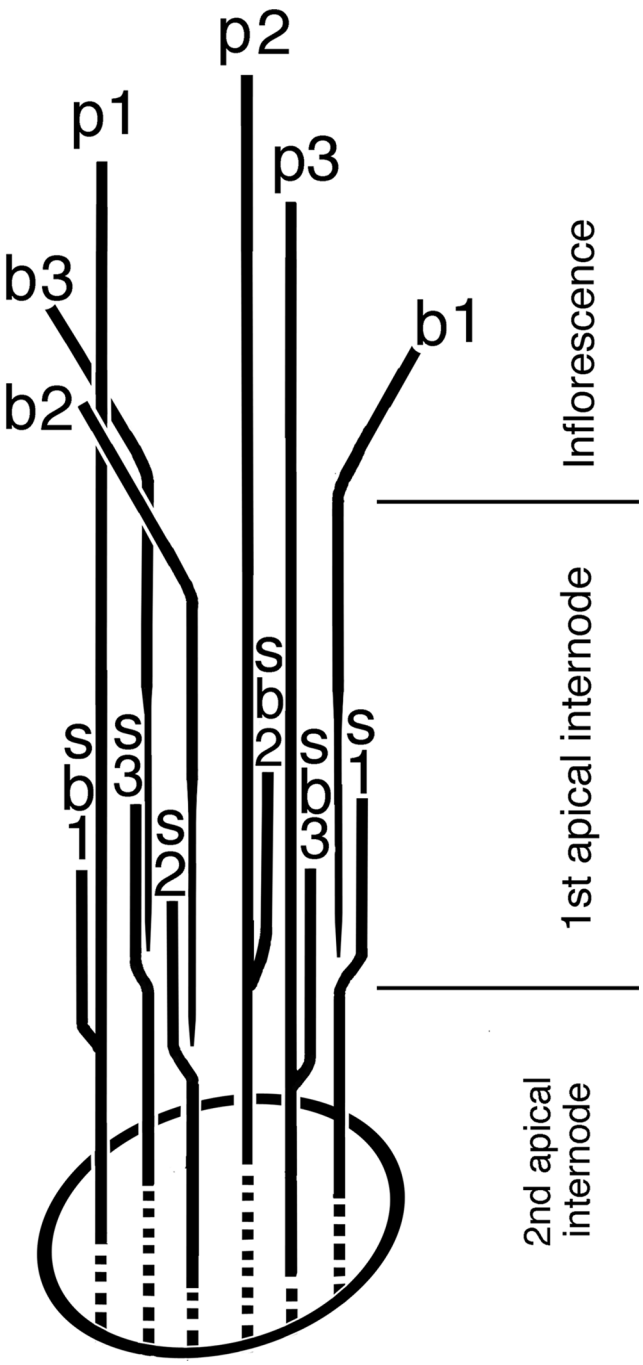


**Fig. 7** A schematic diagram showing three-dimensional reconfiguration of scape vasculature of *Eriocaulon taquetii*. *b1–b3* VB connected to involucral bract, *p1–p3* VB connected to peduncle, *s1–s3* VB connected to spathe, *sb1–sb3* VB branched from *p1–p3* and connected to spathe

**Acknowledgments** We thank Jun Takada (Akita Natural History Society, Japan) for helping us to collect materials. We thank three anonymous reviewers for their helpful comments. This work was partially supported by JSPS KAKENHI Grant number JP26440205 (to Y.E.).

## References

Aloni R (2010) The induction of vascular tissues by auxin. In: Davies PJ (ed) Plant hormones: biosynthesis, signal transduction, action! Kluwer Academic Publishers, Dordrech, pp 471–492

APG IV (2016) An update of the angiosperm phylogeny group classification for the orders and families of flowering plants: APG IV. Bot J Linn Soc 181:1–20

Ayensu ES (1972) Dioscoreales. In: Metcalfe CR (ed) Anatomy of the monocotyledons IV, 182 pp with16 plates, Clarendon Press, Oxford

Bayer EM, Smith RS, Mandel T, Nakayama N, Sauer M, Prusinkiewicz P, Kuhlemeier C (2009) Integration of transport-based models for phyllotaxis and midvein formation. Genes Dev 23:373–384

Bell A (1980) The vascular pattern of a rhizomatous ginger (*Alpinia speciosa* L. Zingiberaceae). 1. The aerial axis and its development. Ann Bot 46:203–212

Bercu R (2005) Contribution to the anatomy of *Sagittaria sagittifolia* L. (Alismataceae). J Biol Res 4:213–215
Blunden G, Binns WW (1970) The leaf anatomy of *Yucca glauca* Nutt. Bot J Linn Soc 63:133–141
Blunden G, Jewers K (1973) The comparative leaf anatomy of *Agave*, *Beschorneria*, *Doryanthes* and *Furcraea* species (Agavaceae: Agaveae). Bot J Linn Soc 66:157–179
Bond J, Donaldson L, Hill S, Hitchcock K (2008) Safranin fluorescent staining of wood cell walls. Biotech Histochem 83:161–171
Bosabalidis AM, Evert RF, Russin WA (1994) Ontogeny of the vascular bundles and contiguous tissues in the maize leaf blade. Am J Bot 81:745–752
Chonan N, Kawahara H, Matsuda T (1974) Morphology on vascular bundles of leaves in gramineous crops I. Observation on vascular bundles of leaf blades, sheaths and internodes in rice plants. Proc Crop Sci Soc Jpn 43:425–432 (in Japanese with English abstract)
Claßen-Bockhoff R, Franke D, Krämer H (2020) Early ontogeny defines the diversification of primary vascular bundle systems in angiosperms. Bot J Linn Soc XX 1–27 with 13 figures
Esau K (1953) Plant anatomy. Wiley, New York
Evans PS (1965) Intercalary growth in the aerial shoot of *Eleocharis acuta* R. Br. Prodr Ann Bot 29:205–217
Fischer JB (1970) Xylem derived from the intercalary meristem of *Cyperus alternifolius*. Bull Torrey Bot Club 97:58–66
Fischer JB, French JC (1976) The occurrence of intercalary and uninterrupted meristems in the internodes of tropical monocotyledons. Am J Bot 63:510–525
Gifford EM, Foster AS (1989) Morphology and evolution of vascular plants, 3rd edn. Freeman WH and company, New York
Givnish TJ, Zuluaga A, Spalink D, Gomez MS, Lam VKY, Saarela JM, Sass C et al (2018) Monocot plastid phylogenomics, timeline, net rates of species diversification, the power of multi-gene analyses, and a functional model for the origin of monocots. Am J Bot 105:1888–1910
Govindarajalu E (1967) Further contribution to the anatomy of the Alismataceae: *Sagittaria guayanensis* H.B.K. ssp. *lappula* (D. Don) Bogin. Proc India Acad Sci – Sect B 65: 142–152
Harb RK, El-Kobisy OS, Desoukey SF (2016) Anatomical and chemical investigations on *Asparagus officinalis* L. (Asparagaceae). Arab Univ J Agric Sci 24:655–664
Hare CL (1945) The structure and development of *Eriocaulon septangulare* With. J Linn Soc Bot 53:422–448
Heywood VH (1978) Flowering plants of the world. Oxford Univ Press, London
Holm T (1901) *Eriocaulon decangulare* L.: An anatomical study. Bot Gaz 31:17–37
Maze J (1977) The vascular system of the inflorescence axis of *Andropogon gerardii* (Gramineae) and its bearing on concepts of monocotyledon vascular tissue. Am J Bot 64:504–515
Nikon Instruments Inc (2020) Fern sorus thin section, G-2A Longpass Emission (Wide Bandwidth Excitation) Green Set. (https://www.microscopyu.com/techniques/fluorescence/nikon-fluorescence-filter-sets/green-excitation-filter-sets/green-excitation-g-2a-longpass-emission), 2020. 5. 30
Oliveira FMG, Scatena VL, Oriani A (2015) Anatomy of vegetative organs and inflorescence axis of *Orectanthe sceptrum* (Xyridaceae–Poales). J Torrey Bot Soc 142:258–268
Pereira RA, Rodrigues AC (2012) Morphoanatomy of the underground stem of *Androtrichum trigynum* (Cyperaceae). Rodriguésia 63:305–319
Povilus RA, DaCosta JM, Grassa C, Satyaki PRV, Moeglein M, Jaenisch J, Xi Z, Mathews S, Gehring M, Davis CC, Friedman WE (2020) Water lily (*Nymphaea thermarum*) genome reveals variable genomic signatures of ancient vascular cambium loses. Proc Nat Acad Sci USA 117:8649–8656
Rodrigues AC, Estelita MEM (2009) Morphoanatomy of the stem in Cyperaceae. Acta Bot Bras 23:889–901
Rudall P (1991) Lateral meristems and stem thickening growth in monocotyledons. Bot Rev 57:150–163
Saikawa M (2016) Not all of the vascular bundles are distributed widely and scattered irregularly throughout the transverse-sectional area of monocotyledonous stem. Bull Tokyo Gakugei Univ Div Nat Sci 68:229–243 (in Japanese with English abstract)
Sajo MG (1999) Systematic vegetative anatomy and ensiform leaf development in *Xyris* (Xyridaceae). Bot J Linn Soc 130:171–182
Scarpella E, Meijer H (2004) Pattern formation in the vascular system of monocot and dicot plant species. New Phytol 164:209–242
Scatena VL, Giulietti AM (1996) The taxonomy and morphological and anatomical differentiation of populations of *Leiothrix crassifolia* (Eriocaulaceae). Plant Syst Evol 199:243–258
Scatena VL, Rosa MM (2001) Morphology and anatomy of the vegetative organs and scapes from *Aphorocaulon* (*Paepalanthus*, Eriocaulaceae). Br Arch Biol Technol 44:49–58
Scatena VL, Giulietti AM, Cardoso VA (1999) Anatomia de raízes, escapos e folhas de espécies de *Eriocaulon* L. (Eriocaulaceae). Bol Bot Univ São Paulo 18:11–20
Scatena VL, Vich DV, Parra LR (2004) Anatomia de escapos, folhas e brácteas de *Syngonanthus* sect. *Eulepis* (Bong. ex Koern.) Ruhland (Eriocaulaceae). Acta Bot Bras 18:825–837
Scatena VL, Giulietti AM, Bolba EL, van den Berg C (2005) Anatomy of Brazilian Eriocaulaceae: correlation with taxonomy and habitat using multivariate analyses. Plant Syst Evol 253:1–22
Sharmann BC (1942) Developmental anatomy of the shoot of *Zea mays* L. Ann Bot 6: 245–282, Plate VII
Sheikh N, Kumar Y (2017) Foliar epidermal, stem and petiole anatomy of Meghalayan *Dioscorea* L. (Dioscoreaceae) and its systematic implication. Bangladesh J Plant Taxon 24:53–63
Stant MY (1964) Anatomy of the Alismataceae. J Linn Soc (Bot) 59:1–42
Stevens PF (2001 onwards) Angiosperm Phylogeny Website. Version 14, July 2017 [and more or less continuously updated since]." will do. http://www.mobot.org/MOBOT/research/APweb/.
Stützel T (1998) Eriocaulaceae. In: The families and genera of vascular plants IV-flowering plants: Monocotyledons-Alismataceae and Commelinaceae (except Gramineae), (ed) Kubitzki K. Springer-Verlag, Berlin, pp 197–207
Takada J (2017) A guide of *Eriocaulon* plants of Japan, 125 pp (in Japanese). Akita Kyodo Printing Co Ltd, Akita
Tan AS, Rao AN (1974) Studies on the developmental anatomy of *Dioscorea sansibarensis* Pax (Dioscoreaceae). Bot J Linn Soc 69:211–227
Tomlinson PB (1969) Commelinales–Zingiberales. In: Metcalfe CR (ed) Anatomy of the Monocotyledons, vol. III, 446 pp. Clarendon Press, Oxford
Tomlinson PB (1995) Non-homology of vascular organisation in monocotyledons and dicotyledons. In: Rudall PJ, Cribb PJ, Cutler DF, Humphries CJ (eds) Monocotyledons: systematic and evolution. Royal Botanic Gardens, Kew, Kew, pp 589–622
Tomlinson PB, Spangler R (2002) Developmental features of the discontinuous stem vascular system in the rattan palm *Calamus* (Arecaceae-Calamoideae-Calamineae). Am J Bot 89:1128–1141
Tomlinson PB, Fisher JB, Spangler RE, Richer RA (2001) Stem vascular architecture in the rattan palm *Calamus* (Arecaceae-Calamoideae-Calaminae). Am J Bot 88:797–809
Vita RSB, Menzes NL, Pellegrini MOO, Melo-de-Pinna GFA (2019) A new interpretation on vascular architecture of the cauline system in Commelinaceae (Commelinales). PLoS ONE 14:e0218383
Zimmermann WH, Tomlinson PB (1965) Anatomy of the palm *Rhapis excelsa* I Mature vegetative axis. J Arnold Arbor 46:160–177

Zimmermann WH, Tomlinson PB (1968) Vascular construction and development in the aerial stem of *Prionium* (Juncaceae). Am J Bot 55:1100–1109

Zimmermann WH, Tomlinson PB (1972) The vascular system of monocotyledonous stems. Bot Gaz 133:141–155